

Hierarchical Structures of $\text{Li}_{1+x}\text{V}_3\text{O}_8$ Nanorods Growing on Electrospun Fibers: Synthesis, Characterization and Electrochemical Properties

BIN YAN, SHUPING WANG, HONGXIAO YANG, LIJUN FENG, HUIYING WEI and YANZHAO YANG*

Key Laboratory for Special Functional Aggregate Materials of Education Ministry, School of Chemistry and Chemical Engineering, Shandong University, Jinan 250100, P.R. China

*Corresponding author: Fax: +86 531 88564464; Tel: +86 531 88365431; E-mail: yzhyang@sdu.edu.cn

(Received: 24 April 2012;

Accepted: 9 February 2013)

AJC-12953

Hierarchical structures of $\text{Li}_{1+x}\text{V}_3\text{O}_8$ nanorods growing on electrospun fibers have been successfully synthesized by electrospinning and calcinations. Field-emission scanning electron microscopy, transmission electron microscopy, X-ray diffraction and Raman spectra are applied to characterize the products. The formation mechanism of the hierarchical structures is investigated, showing that the morphology of the hierarchical structures is mainly determined by calcined conditions, such as temperature and time of calcination. Electrochemical properties of the $\text{Li}_{1+x}\text{V}_3\text{O}_8$ hierarchical structures are investigated by cyclic voltammetry and charge-discharge experiments. The results demonstrate that the $\text{Li}_{1+x}\text{V}_3\text{O}_8$ hierarchical structures exhibited a high discharge capacity (313 mAhg^{-1}) and excellent cycling stability.

Key Words: Hierarchical nanostructures, Lithium vanadate, Electrospinning, Cathode materials.

INTRODUCTION

In recent years, the controllable arrangement of micro- and nano-structured building blocks into hierarchical structures has attracted considerable interest to chemists and materials scientists^{1,2} because the properties of nano- and microcrystals depend not only on their chemical composition, but also on their structure, phase, shape and size. Such complex architectures, especially those based on one-dimensional nanostructures, are expected to display novel properties and may have potential applications in many fields such as catalysis, cosmetic, battery and medicine³. Many efforts have been put on the fabricating these architectures and a number of different approaches such as chemical vapor deposition⁴, laser-assisted catalytic growth⁵, template-based design techniques⁶ and solution-based self-assembly routes⁷ have been developed.

As a simple and versatile technique for generating ultra thin fibers, electrospinning was further extended to fabricate complex nanostructures with controllable hierarchical architectures⁸⁻¹². For example, a novel hierarchical structure of V_2O_5 nanorods on TiO_2 nanofibers was made by electrospinning¹³, nanofibers with hollow, core-shell or porous structures have also been synthesized through modifying electrospinning setup or adjusting the spinning parameters^{14,15}. $\text{Li}_{1+x}\text{V}_3\text{O}_8$ is one of the promising cathode materials in rechargeable lithium batteries, have been extensively studied due to attractive characteristics such as high specific capacity, good rate capacity and

long cycle life^{16,17}. But, no attempts have been made so far to prepare hierarchical structures of $\text{Li}_{1+x}\text{V}_3\text{O}_8$ nanorods growing on electrospun fibers for attaining good performance. In this report, hierarchical structures of $\text{Li}_{1+x}\text{V}_3\text{O}_8$ nanorods growing on electrospun fibers were fabricated through electrospinning and calcinations. The electrochemical properties of the as-prepared $\text{Li}_{1+x}\text{V}_3\text{O}_8$ hierarchical architectures were investigated and the results exhibited the $\text{Li}_{1+x}\text{V}_3\text{O}_8$ hierarchical architecture with high capacities and excellent cycling reversibility, which indicates their promising features for applications as electrode materials in advanced rechargeable lithium ion batteries.

EXPERIMENTAL

Preparation of $\text{Li}_{1+x}\text{V}_3\text{O}_8$ fibers: All chemicals were of analytical grade and were used as received without further purification. Sol-gel method was used to prepare the electrospinning solution. In a typical experiment, 0.0105 mol lithium acetate monohydrate and 0.04 mol citric acid were dissolved in 50 mL distilled water and 0.03 mol NH_4VO_3 was added into 80 mL distilled water. Then the former solution was added to the NH_4VO_3 under stirring and NH_4VO_3 began to dissolve slowly with the addition of citric acid until it got salmon pink solution. The colour of the solution became deeper during the stirring process and turned to navy blue finally. Then the mixture was kept at 70 °C to turn into a viscous sol to form a sol with viscosity of 3.0 Pa·S. The sol was then loaded into a Teflon bushing equipped with a spinneret made of

stainless steel (the aperture is 400 mm), which was connected to a high-voltage supply (BGG-80 kV/20 mA). When the intensity of electric field was high enough, a charged sol jet was ejected from the spinneret to form a fiber-like product that fell on the collector and was then dried to remove volatile components. The obtained xerogel fibers were first heated at 400 °C for 2 h in air with a heating rate of 0.5 °C min⁻¹ and then heated at 550 °C for 8 h at the heating rate of 2.0 °C min⁻¹ from 400 to 550 °C.

The morphology of fibers was investigated by a JEOL JSM-6700F field-emission scanning electron microscopy (FE-SEM Hitachi S-520) and transmission electron microscopy (TEM, model H-800). X-ray diffraction patterns of product were examined using a Rigaku D/Max 2200 PC diffractometer with a graphite monochromator and CuK_α radiation ($\lambda = 0.15418$ nm) while the voltage and electric current were held at 40 kV and 20 mA ($2\theta = 10\sim 80^\circ$). Raman spectra were collected at room temperature using a Jobin-Yvon ISA U1000 Raman spectrometer in a quasi-backscattering configuration, the wavelength of the Ar laser was 514.5 nm. BET surface area was performed on SSA-3500 micromeritics using the N₂ adsorption-desorption method.

Electrochemical properties of the Li_{1+x}V₃O₈ hierarchical structures: Electrochemical measurements were carried out using laboratory cells. The fiber electrode was fabricated by loading the fibers into a bag made up of a stainless steel net and they were subjected to a pressure of 12.0 MPa. Fresh lithium foil was used as reference and counter electrodes. The electrolyte consisted of 1 M LiPF₆ in a non-aqueous solution of ethylene carbonate and dimethyl carbonate at a volume ratio of 1:1. Cyclic voltammograms were obtained at a scanning rate of 0.1 mV s⁻¹ between 0.01 and 3.0 V. Charge/discharge characteristics of the cells were recorded at a current density of 50 mA g⁻¹.

RESULTS AND DISCUSSION

The phase composition and purity of the products were characterized by XRD analysis. Fig. 1a illustrates the XRD patterns of the Li_{1+x}V₃O₈ hierarchical structures. All of the diffraction peaks of XRD pattern of the Li_{1+x}V₃O₈ hierarchical structures could be well indexed to the monoclinic structure with the unit cell parameters of $a = 6.680$ Å, $b = 3.595$ Å, $c = 12.036$ Å, which was in agreement with the layered Li_{1+x}V₃O₈ (JCPDS file No.72-1193). The Raman spectrum of hierarchical

structures was shown in Fig. 1b. The characteristic adsorption of Li_{1+x}V₃O₈ hierarchical structures at 987 cm⁻¹ were assigned to the two vanadyl bonds in VO₆ while the band at 767 cm⁻¹ was attributed to the atomic motion of corner-sharing oxygen among the VO₆, VO₅ and LiO₆ polyhedrons¹⁸.

Fig. 2 provides the direct information of microstructures and morphologies of the Li_{1+x}V₃O₈ hierarchical structures at low and high magnifications, respectively. The low magnification (Fig. 2a) FE-SEM image revealed that the products consisted of a large quantity of 3-D hierarchical structures with a major core structure and secondary rods grown on the surfaces of the Li_{1+x}V₃O₈ fibers. As shown in Fig. 2b, the length of major core fibers along the axis could be as long as tens of micrometers and the diameter was about 1-2 μm, whereas the length of the secondary nanorods growing on the major core fibers was in the range of 1-5 μm, with diameters ranging from 100 to 300 nm. The fibers were placed in deionized water and treated ultrasonically. The corresponding SAED pattern (Fig. 2c) of the nanorod indicated a preferential growth [010] of the nanorod.

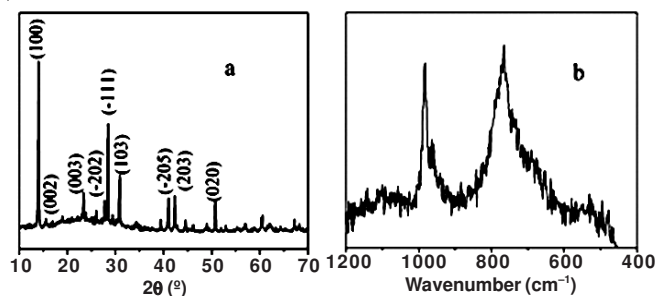


Fig. 1. XRD pattern (a) and Raman spectrum (b) of Li_{1+x}V₃O₈ hierarchical structures

To shed light on the formation mechanism of novel Li_{1+x}V₃O₈ hierarchical structures, we tracked the evolution of their growth process by examining the products harvested at different intervals of calcined times. The resulting morphology was dependent on calcined conditions. The obvious evolutionary stages could be clearly observed and were shown in Fig. 3. The gel fibers were calcined at 550 °C in air for 4 h, only simple Li_{1+x}V₃O₈ fibers could be obtained (Fig. 3a). As the calcinations proceeded, however, new features started to evolve on the surface of the fibers. After the as-spun fibers have been calcined for 6 h, the surface of the fibers became rough and

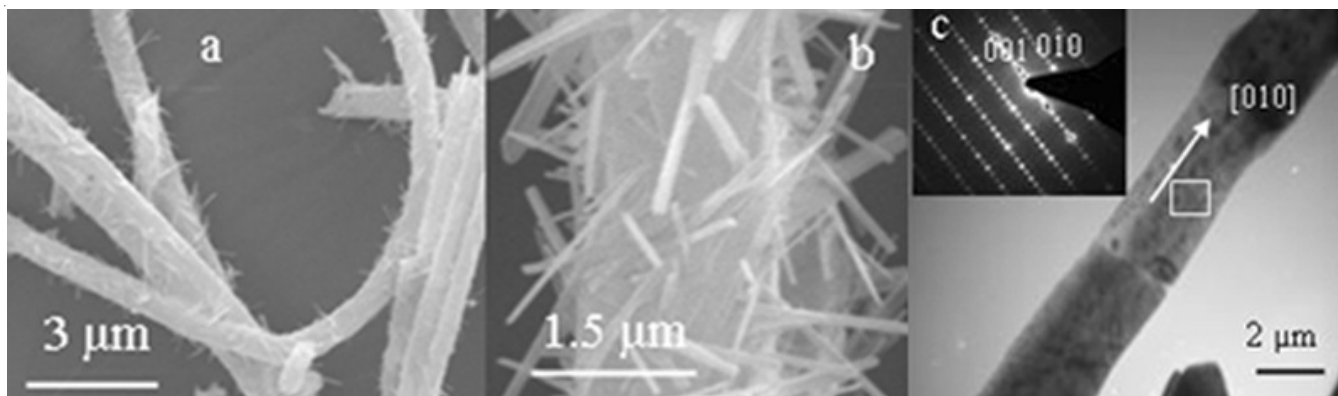


Fig. 2. (a) low-magnification, (b) high-magnification FE-SEM images and (c) selective area electron diffraction of Li_{1+x}V₃O₈ hierarchical structures

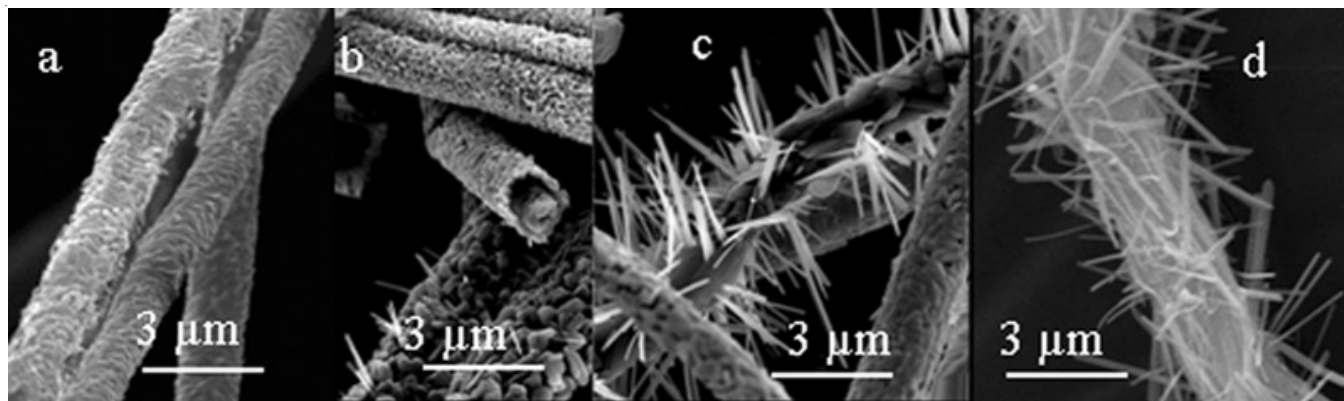


Fig. 3. FE-SEM images of $\text{Li}_{1+x}\text{V}_3\text{O}_8$ hierarchical structures after calcined at 550 °C for (a) 4 h, (b) 5 h, (c) 6 h and (d) 8 h

short nanorods with a smooth surface appeared on the fibers. The surface of the fibers became rougher and the number of nanorods increased as prolonging the time of calcination. The growth of nanorods was fast at the beginning of calcination, slowed after about 1 h and finally stopped after several hours. Temperature-dependent experiments indicated that the calcination temperature also significantly affected the formation of the $\text{Li}_{1+x}\text{V}_3\text{O}_8$ hierarchical structures. It demonstrated that when the sample was calcined below 550 °C, only simple $\text{Li}_{1+x}\text{V}_3\text{O}_8$ fibers could be formed. With the calcined temperature rising to 580 °C, the rods composing the fibers grew further. When the fibers were sintered at 600 °C, the fibers fused and could not keep the fiber morphology. On the basis of the above experimental results, we proposed the growth of $\text{Li}_{1+x}\text{V}_3\text{O}_8$ hierarchical structures was controlled by thermodynamics through increasing the reaction temperature and prolonging the reaction time. $\text{Li}_{1+x}\text{V}_3\text{O}_8$ is monoclinic structure and belongs to the $\text{P}2_1/m$ space group, which is composed of two basic structural units including a VO_6 octahedron and a VO_5 distorted trigonal bipyramids¹⁹. According to previous reports¹⁸⁻²⁰, the $\text{Li}_{1+x}\text{V}_3\text{O}_8$ particles are preferential to form the nanorods at higher temperature due to its structure. Because of the confinement of the particles composed of the fibers, the growth of particles is always interfered by others, leading to that the calcined fibers are mostly composed of sheet-like particles. However, there are always some of particles, especially particle in the fiber surface, have enough area to make their growth be capable to expand spatially. Therefore, the nanorods with a smooth surface appeared on the fibers in the process of calcinations. Finally, the 3-D hierarchical structures with a major core structure and secondary rods growing on the site surfaces of the $\text{Li}_{1+x}\text{V}_3\text{O}_8$ fibers were formed.

Typical cyclic voltammograms of the $\text{Li}_{1+x}\text{V}_3\text{O}_8$ hierarchical structures were shown in Fig. 4a. The main cathodic peaks and one anodic peak were observed in the cyclic voltammogram curve, which indicated the complicated multistep lithium intercalation processes. Compared to the first cyclic voltammogram curve, the second cyclic voltammogram curve displayed a large decrease of the peak intensity. After the 3th cycle, the area and shape of the cyclic voltammogram curves for $\text{Li}_{1+x}\text{V}_3\text{O}_8$ hierarchical structures exhibited very small changes, which indicated that the lithium-ion intercalation and de-intercalation became easier due to the fully

wetting of the electrode and should support good cyclic stability. Charge-discharge experiments were carried out to investigate the electrochemical properties of the $\text{Li}_{1+x}\text{V}_3\text{O}_8$ products and the charge-discharge curve was given in Fig. 4b. In the first cycle, $\text{Li}_{1+x}\text{V}_3\text{O}_8$ hierarchical structures delivered highly initial discharge capacity of *ca.* 313 mAhg^{-1} , the capacity decreased to *ca.* 246 mAhg^{-1} after 40 cycles. The hierarchical structures of $\text{Li}_{1+x}\text{V}_3\text{O}_8$ products had high BET surface area of 8.54 m^2g^{-1} , which led to a short diffusion distance of the Li^+ cations and was beneficial to the intercalation/deintercalation of Li^+ cations^{21,22}. On the other hand, the hierarchical structures of $\text{Li}_{1+x}\text{V}_3\text{O}_8$ products might offer a continuous electronic pathway, yielding an electronic conductivity of reasonable magnitude for Lithium batteries, in which the geometry of the fibers maximizes the solid-solution interfacial contact and results in increased charging rates. Therefore, the fiber materials presented high charge-discharge capacities and better cycle performance.

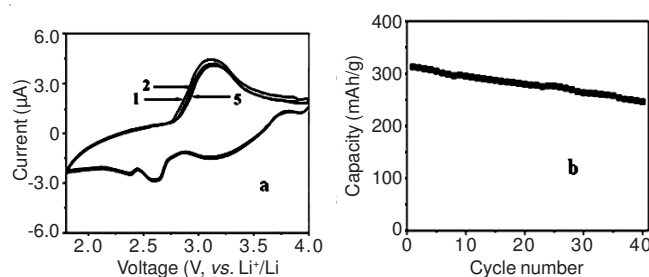


Fig. 4. Cyclic voltammograms and variation of discharge capacity as a function of cycle number using the $\text{Li}_{1+x}\text{V}_3\text{O}_8$ hierarchical structures.

Conclusion

3D hierarchical structures with a major core structure and secondary rods growing on the site surfaces of the $\text{Li}_{1+x}\text{V}_3\text{O}_8$ fibers were fabricated by using a single spinneret electrospinning technique combined with sol-gel method. The growth of $\text{Li}_{1+x}\text{V}_3\text{O}_8$ hierarchical structures was controlled by thermodynamics through controlling the reaction temperature and adjusting the reaction time. As electrode materials, the $\text{Li}_{1+x}\text{V}_3\text{O}_8$ hierarchical structures exhibited a high discharge and a good electrochemical performance. Therefore, the $\text{Li}_{1+x}\text{V}_3\text{O}_8$ hierarchical structures could be a promising model system as cathode materials in lithium-ion batteries.

ACKNOWLEDGEMENTS

The authors acknowledged the financial support for this work from the National Natural Science Foundation of China (No. 21076115), the Major State Basic Research Development Program of China (No. 2011CB935901).

REFERENCES

1. L.J. Lauhon, M.S. Gudiksen, C.L. Wang and C.M. Lieber, *Nature*, **420**, 57 (2002).
2. Z. Yao, X. Zhu, C. Wu, X. Zhang and Y. Xie, *Cryst. Growth Design*, **7**, 1256 (2007).
3. Y. Li, J. Liu, X. Huang and G. Li, *Cryst. Growth Design*, **7**, 1350 (2007).
4. A.C. Chen, X.S. Peng, K. Koczkur and B. Miller, *Chem. Commun.*, **17**, 1964 (2004).
5. A.M. Morales and C.M. Lieber, *Science*, **279**, 208 (1998).
6. X.F. Duan and C.M. Lieber, *Adv. Mater.*, **12**, 298 (2000).
7. Y. Li, D. Xu, Q. Zhang, D. Chen, F. Huang, Y. Xu, G. Guo and Z. Gu, *Chem. Mater.*, **11**, 3433 (1999).
8. G. Cheng, J. Wang, X. Liu and K. Huang, *J. Phys. Chem. B*, **110**, 16208 (2006).
9. Z. Liu, D.D. Sun, P. Guo and J.O. Leckie, *Nano Lett.*, **7**, 1081 (2007).
10. D. Li, J.T. McCann and Y. Xia, *Small*, **1**, 83 (2005).
11. D. Li, Y. Wang and Y. Xia, *Adv. Mater.*, **16**, 361 (2004).
12. D. Li, G. Ouyang, J.T. McCann and Y. Xia, *Nano Lett.*, **5**, 913 (2005).
13. R. Ostermann, D. Li, Y. Yin, J.T. McCann and Y. Xia, *Nano Lett.*, **6**, 1297 (2006).
14. D. Li and Y. Xia, *Nano Lett.*, **4**, 933 (2004).
15. J.T. McCann, D. Li and Y. Xia, *J. Mater. Chem.*, **15**, 735 (2005).
16. F. Bonino, S. Panero, M. Pasquali and G. Pistoia, *J. Power Source*, **56**, 193 (1995).
17. H. Xu, H. Wang, Z. Song, Y. Wang, H. Yan and M. Yoshimura, *Electrochim. Acta*, **49**, 349 (2004).
18. G. Yang, G. Wang and W. Hou, *J. Phys. Chem. B*, **109**, 11186 (2005).
19. S. Jounaneau, A.L. La Salle, A. Verbaere, M. Deschamps, S. Lascaud and D. Guyomard, *J. Mater. Chem.*, **13**, 921 (2003).
20. Y. Gu and F. Jian, *J. Sol-gel. Sci. Technol.*, **46**, 161 (2008).
21. S. Zhang, W. Li, C. Li and J. Chen, *J. Phys. Chem. B*, **110**, 24855 (2006).
22. B. Li, G. Rong, Y. Xie, L. Huang and C. Feng, *Inorg. Chem.*, **45**, 64040 (2006).